

# Experimental Coexistence Investigation of Distributed Acoustic Sensing and Coherent Communication Systems

Zhencheng Jia, L. Alberto Campos, Mu Xu, Haipeng Zhang

Cable Television Laboratories Inc., 858 Coal Creek Circle, Louisville, CO 80027, USA. [s.jia@cablelabs.com](mailto:s.jia@cablelabs.com)

Miguel Gonzalez-Herraez

Department of Electronics, University of Alcalá, Alcalá de Henares 28805, Spain, [miguel.gonzalez-h@uh.es](mailto:miguel.gonzalez-h@uh.es)

Hugo F. Martins

Institute of Optics "Daza de Valdés" (IO-CSIC), 28006 Madrid, Spain. [hugo.martins@csic.es](mailto:hugo.martins@csic.es)

Zhongwen Zhan

Seismological Laboratory, California Institute of Technology, Pasadena, CA 91125, USA. [zwzhan@gps.caltech.edu](mailto:zwzhan@gps.caltech.edu)

**Abstract:** We demonstrate the co- and counter-propagation coexistence of distributed acoustic sensing and 100G/200G coherent data communication over a single fiber, proving ubiquitous and practical sensing through pervasive telecom fiber infrastructure. © 2021 The Author(s)

## 1. Introduction

During the past decade, the field of distributed fiber optic sensing (DFOS) has attracted significant attention globally for measuring strain, temperature and vibration over long distances by utilizing the backscattered Rayleigh, Raman, or Brillouin signals. Among DFOS, distributed acoustic sensing (DAS) is particularly interesting as it allows the distributed monitoring of vibrations along an optical fiber cable with extremely high sensitivity. In a wide range of potential applications, DAS has created a paradigm shift in applied geophysics by enabling arrayed seismic measurements at high sampling frequency (up to kHz), large distances (typically tens of kilometers), and fine spatial sampling resolution (in the meter scale) at a reasonable cost. Recently, several demonstrations of seismic monitoring utilizing different DAS techniques have been reported over installed dark fiber [1,2,3,4]. However, employing dark fiber for this application implies reserving the full fiber strand for the DAS operation (usually comprising only one-wavelength signaling), which is very inefficient and uneconomical for wide scale deployment of sensing networks. Moreover, the huge capacity demand for optical fiber has caused a shortage in certain regions, which will only intensify as fiber demand for business and wireless backhaul increases and fiber deep architectures become prevalent. In most cases, fiber retrenching is extremely costly and should be avoided. It is therefore critical to use the existing optical fiber infrastructure more efficiently. The coexistence of both data and sensing information on the same fiber offers the most powerful and cost-effective solution by additionally turning entire networks into distributed sensing systems. However, the fact is that sensing signals used in the common time-domain DAS schemes have a much higher power density in a short period of time than typical coherent communication signals, causing them to have a much greater impact on the refractive index for nonlinear effects.

In this paper, we explore the coexistence of a high-fidelity distributed acoustic sensing (HDAS) channel and 100G/200G coherent optical channels on the same optical fiber. We analyze the requirements for coexistence, including spectrum allocation, power level control, sensing pulse configuration, and relative direction of data and sensing signals in DWDM systems. The conditions and system parameters, for which coexistence is guaranteed, are provided for the first time to the best of our knowledge.

## 2. HDAS Operation Principle

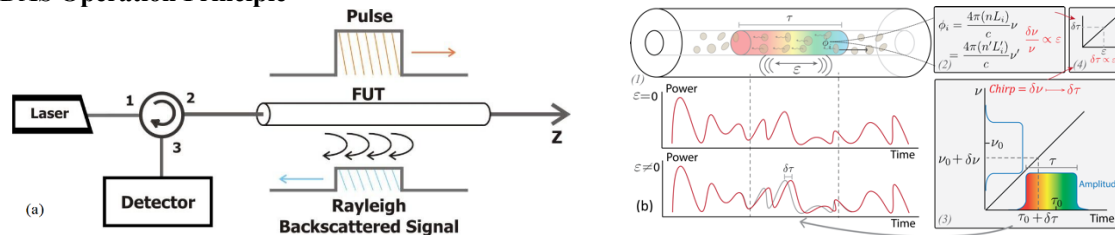


Fig. 1. (a) Conceptual DAS operation. (b) Working principle of chirped-pulse DAS (CP-ΦOTDR).

The HDAS operation is based on chirped-pulse DAS [4,5]: a modified version of phase-sensitive OTDR (ΦOTDR) using chirped pulses (CP-ΦOTDR). In its simplest form, the technique relies on launching coherent optical pulses into a fiber and monitoring the Rayleigh backscattered pattern via the same fiber end (Fig. 1a). Perturbations along

the fiber (temperature, strain/vibrations or refractive index variations) change the optical path distance between the fiber scattering centers, thus changing the resulting backscattered interference pattern. Since these changes can be compensated by a frequency detuning of the pulse central frequency, the use of linearly chirped pulses maps these perturbations into a local temporal delay of the optical trace, that can be monitored with direct detection (Fig. 1b). The working principle is therefore fundamentally different from traditional DAS, with important advantages: owing to the use of direct detection the technique is intrinsically immune to blind spots caused by interference fading, as well as polarization fading, whilst maintaining a linear and higher sensitivity to applied perturbations. The acoustic noise variability from point to point can therefore be orders of magnitude below those of traditional coherent detection ΦOTDR [4], while maintaining relaxed specs on detection and laser requirements. Typical operation in seismic sensing for long fiber (i.e., >~20 km) yields pulses with few kHz repetition rate (i.e., acoustic sampling) and 10ns - 100ns width (i.e., 1meter - 10meters spatial resolution) with a peak power that is limited to ~200mW, due to the onset of nonlinearities during pulse propagation. Current applications of DAS to pre-existing telecom dark fibers in urban environment have demonstrated remarkable sensitivity and data fidelity. As an example, Fig.2a shows the DAS records of the August 19, 2018 Magnitude 8.2 Tonga earthquake on a DAS array 8000 km away in the city of Pasadena, California [2]. Comparison of the travel times and waveforms with co-located conventional seismometers show good consistency over multiple frequency bands. Therefore, HDAS has proven to be able to convert telecom dark fibers into highly sensitive geophysical sensor arrays.

### 3. Coexistence Experimental Setup

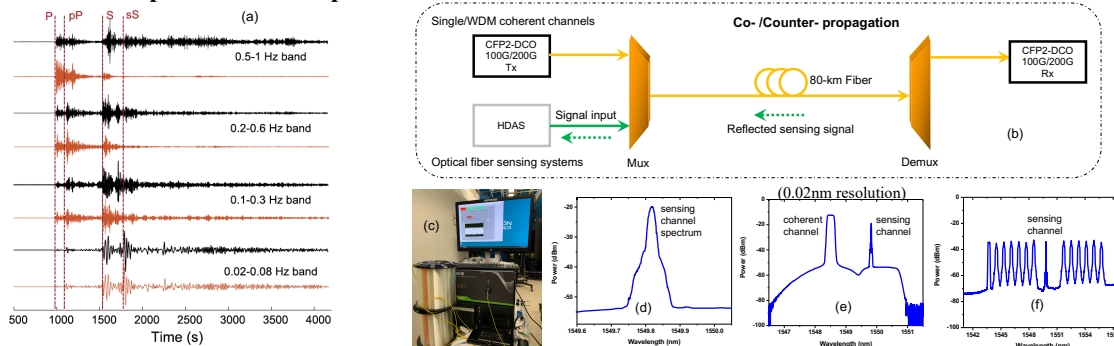


Fig. 2. (a) Comparison of DAS records of an earthquake with co-located conventional seismometer in a few frequency bands between 0.02Hz and 1Hz, (b) Coexisting optical system experimental setup, (c) HDAS equipment and software platform, (d) the individual sensing spectrum, (e) coexisting spectra with single coherent channel, and (f) coexisting spectra with WDM channels.

The experimental setup for the coexisting fiber sensing system and data transmission is shown in Fig. 2b. The CFP2-DCO transceiver module is employed for single coherent channel connection [6]. It supports 100Gb/s client data rate using 31.4Gbaud PM-QPSK and 200Gb/s client data rate using 31.4Gbaud PM-16QAM. In the case of WDM operation, multiple loading coherent channels are generated via discrete coherent setups that consist of external-cavity lasers (ECLs), quad-parallel modulators, integrated RF drivers, and arbitrary waveform generator (AWG). The HDAS pulses had a repetition rate of 1 kHz, an optical intensity profile of a super-Gaussian with FWHM of 20ns-100 ns (1E-4 duty cycle) and 500 MHz frequency (chirp) content. The system was calibrated to ensure that the pulses' peak powers (software programmable) had between 20mW-200mW when entering the fiber, i.e., after accounting for the Mux losses. Considering a typical -82dB/ns fiber Rayleigh backscattering coefficient, the generated CW backscattering pattern is expected to have an average power of ~10nW -100 nW, before accounting for fiber propagation losses. This HDAS photo is shown in Fig. 2c. The generated optical spectrum of this high-power chirped pulses is shown in Fig. 2d. The communication channels and the fiber sensing signal are combined via the optical mux and then travel through the same fiber. The corresponding optical spectra for single channel and WDM operation are shown in Fig.2e and Fig.2f respectively. The coexistence was tested in co-propagation and counter-propagation [7] to investigate the impact of nonlinearity crosstalk.

### 4. Experimental Results

Fig. 3 presents the experimental results over 80-km fiber transmission distance. Because of the fiber nonlinearity crosstalk introduced by ultra-high instantaneous sensing pulse power, error floors were observed for the PM-QPSK signals Fig. 3a and Fig. 3b at levels between 1E-4 and 1E-6 of BER, depending on the sensing pulse peak power. Regarding the PM-16QAM signals in Fig. 3c, the crosstalk-introduced error floor was not observed due to the lower back-to-back sensitivity curves (around 1E-3 of BER). Channel spacing (from ITU grid 48 to 60) and differential and non-differential configurations of QPSK signals were also carried out in the experiment.

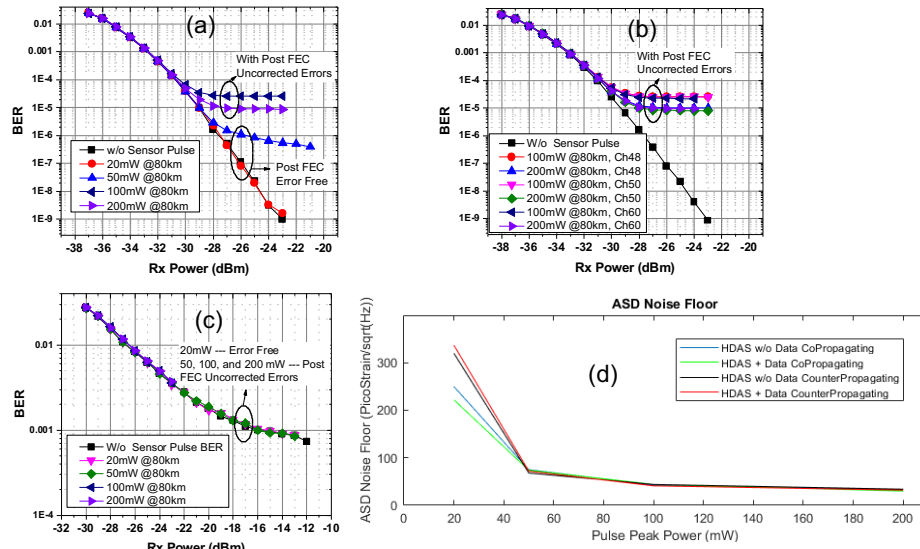


Fig. 3. Coherent channel pre- and post-FEC BER results in coexisting setup (a)single-channel PM-QPSK with sensing signal (b) PM-QPSK WDM channels with sensing signal (c) single-channel PM-16QAM with sensing signal (d) HDAS acoustic noise floor for pulses of 100 ns FWHM with peak powers of 20/50/100/200 mW.

As for the fluctuations of HDAS performance (characterized by acquiring 1 minute of HDAS acoustic signal) for different coexisting scenarios, these were observed to be negligible. The acoustic noise floor remained constant (and consistent with HDAS expected instrumental noise: an amplitude spectral density (ASD) of a few tens of  $\text{picoStrain}/\sqrt{\text{Hz}}$ ) for all combinations. An example of such characterization is presented in Fig. 3d. Note that for the case of 20 mW peak power, fluctuations of instrumental noise floor of up to 3 dB were recorded owing to the existence of random outliers (explained by the HDAS low power of operation and additional Mux losses), but, in any case, these were random and uncorrelated to the data signals.

The summarized results of coexistence measurement are shown in Table 1. For each case, the pre-FEC BER average and post-FEC error count over 1-minute intervals were read from the transceiver. Long-term stability after 80-km transmission was tested by monitoring BER before and after FEC as well. It is noted that counter-propagation works for all different testing scenarios while co-propagation has a strict requirement on pulse power and duration. The cases that are not allowing coexistence means the uncorrected signal blocks appear and post-FEC errors exist.

Table 1. Coexistence summary for PM-QPSK/16QAM signals

Transmission Direction	PM-QPSK	PM-16QAM
Co-propagation	<ul style="list-style-type: none"> <li>Allowed coexistence: (25mW, 100ns), (50mW, 100ns), (75mW, 20ns)</li> <li><b>NOT allowed coexistence:</b> any pulse duration with power <math>\geq 100\text{mW}</math></li> </ul>	<ul style="list-style-type: none"> <li>Allowing coexistence: (25mW, 100ns)</li> <li><b>NOT allowing coexistence:</b> any pulse duration with power <math>\geq 50\text{mW}</math></li> </ul>
Counter-propagation	Allowed coexistence for all testing scenarios	

#### 4. Conclusions

Experimental coexistence investigation of high-fidelity distributed acoustic sensor (HDAS) channel and 100G/200G coherent optical channels over 80-km fiber was conducted. Measurements including power level, pulse duration, relative transmission direction were carried out to provide successful coexistence conditions. A most powerful solution is demonstrated by augmenting sensing functionality to telecommunication networks, leveraging only a fraction of the fiber spectrum to introduce distributed sensors. Accessing many fibers and sharing resources in time offer drastic cost reduction, making sensing for seismic and other use cases ubiquitous and always available.

**Acknowledgement:** The HDAS equipment was provided by Aragon Photonics.

#### 5. References

- [1]. Z. Zhan, Seismological Research Letters 91, no. 1, (2019).
- [2]. M.R. Fernández-Ruiz, APL Photon. 5, 030901 (2020).
- [3]. E.F. Williams *et al*, Nat Commun 10, 5778 (2019).
- [4]. M.R. Fernández-Ruiz *et al*, Sensors, 19, 4368 (2019).
- [5]. J. Pastor-Graells *et. al*, J. Lightwave Technol., vol. 35, no. 21, pp. 4677–4683, (2017).
- [6]. Z. Jia *et al*, OFC 2020, paper Th3A.2.
- [7]. G. A. Wellbrock *et al*, OFC 2019, paper Th4C.